Rea, D.K., Basov, I.A., Scholl, D.W., and Allan, J.F. (Eds.), 1995
Proceedings of the Ocean Drilling Program, Scientific Results, Vol. 145

44. *DATA REPORT:* GEOCHEMISTRY OF VOLCANIC ASHES RECOVERED FROM HOLE 887A[1]

L.-Q. Cao,[2] R.J. Arculus,[2,3] and B.C. McKelvey[2]

ABSTRACT

A total of 25 samples from 82 ash layers interbedded with middle Miocene to recent diatomaceous (variably calcareous) oozes and silty clays overlying Oligocene igneous basement was recovered from Ocean Drilling Program Hole 887A on the Patton-Murray seamount platform in the Gulf of Alaska, northeast Pacific. The ashes consist predominantly of elongate (≈≥5 to ≈<150 µm), tubular, and bubble-wall fragments probably derived from plinian eruption cloud fallout. Major element compositions determined by electron microprobe analysis of individual vitric shards are tholeiitic and bimodal, with predominant medium-K andesite and medium- to high-K rhyolite groups. There is no evidence from this sample set for consistent temporal geochemical changes. High Ba/Nb and Sm/Ti of these ash samples are similar to island-arc magmas in general. Chondrite-normalized La of 40 to 100, Yb of 15 to 30, and La/Yb of about 2 to 3 are similar to tholeiitic volcanic rock series of the Aleutian arc. A major increase in the number of ash layers with depth in the core occurs interlayered with sediments younger than 2.7 Ma.

INTRODUCTION

Initial analytical results are presented here of an ongoing geochemical study of volcanic ash layers interlayered with middle Miocene to Quaternary sediments, which were recovered from Ocean Drilling Program (ODP) Hole 887A (54°22′N, 148°27′W) in the Gulf of Alaska, overlying the Patton-Murray platform (Fig. 1). Hole 887A is located ~≥600 km from the Aleutian-Alaskan island arc. Although the prevailing low-altitude winds are unlikely to have transported ash to the south of this arc system, we know that major plinian eruptions can distribute ash in directions that oppose the low-altitude wind circulation (Carey and Sigurdsson, 1980). Furthermore, Cambray et al. (1993) have shown that representative records of activity can be obtained over time periods of 100 ka on either side of island-arc systems, albeit moderated in terms of total thickness accumulations. We note that the thickness of the individual ash layers at Site 887 is generally ≤10 cm compared with ≤70 cm thick at Deep Sea Drilling Project (DSDP) Site 183 (52°34′N, 161°12′W) (Creager, Scholl, et al., 1973) in the western Gulf of Alaska, which is located at about 150 km from the active subaerial arc. At both sites, the maximum thickness of individual ash layers is significantly less than the ≤250-cm-thick layers recovered from the Detroit Seamount sites (882–884) located some 600 km off the coast of Kamchatka.

We examine the first-order major and trace element compositional changes represented by these ashes during some 15 Ma of arc history. Unfortunately, drilling did not recover volcanic ashes bracketing the period of consumption of the Kula Ridge at ~30 Ma beneath the Aleutian arc.

PREVIOUS STUDIES

The petrogenesis of the Aleutian arc system has been the subject of intensive investigations over the past 30 yr, since the pioneering studies by Coats (1962). There have been vigorous debates concerning the origins of the primary basalt (and andesite) magmas involved (Marsh and Carmichael, 1974; Kay, 1978; Baker and Eggler, 1983; Myers et al., 1985; Brophy and Marsh, 1986; Nye and Reid, 1986; Gust and Perfit, 1987; Myers, 1988; Brophy, 1989), the contributions of different source components, parameters that might control the occurrence of tholeiitic vs. calcalkaline fractionation trends (Kay et al., 1982; Morris and Hart, 1983; Kay and Kay, 1985; Myers et al., 1985; Singer and Myers, 1990; Miller et al., 1992), and the evolution of individual volcanic centers (Nye and Turner, 1990; Romick et al., 1990; Singer et al., 1992). The arc is composed for the most part of a single, narrowly distributed but segmented (Marsh, 1979; Kay et al., 1982; Geist et al., 1988; Singer and Myers, 1990) magmatic trace with only minor development of across-strike, alkalic volcanism.

Studies of the distal record of volcanic activity of the Aleutian arc have previously centered on DSDP Sites 178 and 183 in the Gulf of Alaska (e.g., Scheidegger and Kulm, 1975; Scheidegger et al., 1980). Previous studies have claimed that the composition of the volcanic rocks erupted throughout the Alaskan Peninsula and Aleutians during the Cenozoic, has changed through time (Scheidegger and Kulm, 1975; Edsall, 1976; Scheidegger et al., 1980). The primary observations are (1) that ashes become more silicic through to the Quaternary; (2) an evolution claimed by Edsall (1976) from tholeiitic to andesitic composition during the past 8 Ma, although the other authors cited argue there is no evidence for consistent secular variations in composition; noting however (3), that there are periods when either calcalkaline or tholeiitic magmas predominate. In the case of Site 178, a cyclic variation of SiO_2 content through time was noted.

STRATIGRAPHY AND LITHOLOGY

In Table 1, the summary of the stratigraphic and lithologic characteristics of the ash layers from Hole 887A lists the occurrences of all the ash layers reported in the *Initial Reports* volume (numbered from shallow to deep), identifies the layers sampled for geochemical analysis with a University of New England (UNE) number used in the other tables to identify specific ash layers, and reports ages for the ash layers determined by interpolation of the shipboard micropaleontology, magnetostratigraphy and the calculated sediment mass accumulation rates from Rea, Basov, Janecek, Palmer-Julson, et al. (1993), thickness of ash layers, dimensions of vitric shards, standard (Munsell) color estimated by us for the clay-free, dried, analyzed ash samples, Munsell colors (where reported by the shipboard scientists) for ash layers in the wet cores, volcanic rock type based on our major element analyses, and the nature of the lithologies bounding the ashes.

Rea, Basov, Janecek, Palmer-Julson, et al. (1993) identified a major increase in the number and thickness of the ash layers in sediments younger than about 2.7 Ma, a paucity of layers in sediments between ≈5 and 7.5 Ma, and few ash layers in older sediments.

[1] Rea, D.K., Basov, I.A., Scholl, D.W., and Allan, J.F. (Eds.), 1995. *Proc. ODP, Sci. Results,* 145: College Station, TX (Ocean Drilling Program).
[2] Department of Geology and Geophysics, University of New England, Armidale, NSW 2351, Australia.
[3] Present address: Department of Geology, Australian National University, Canberra, ACT 0200, Australia.

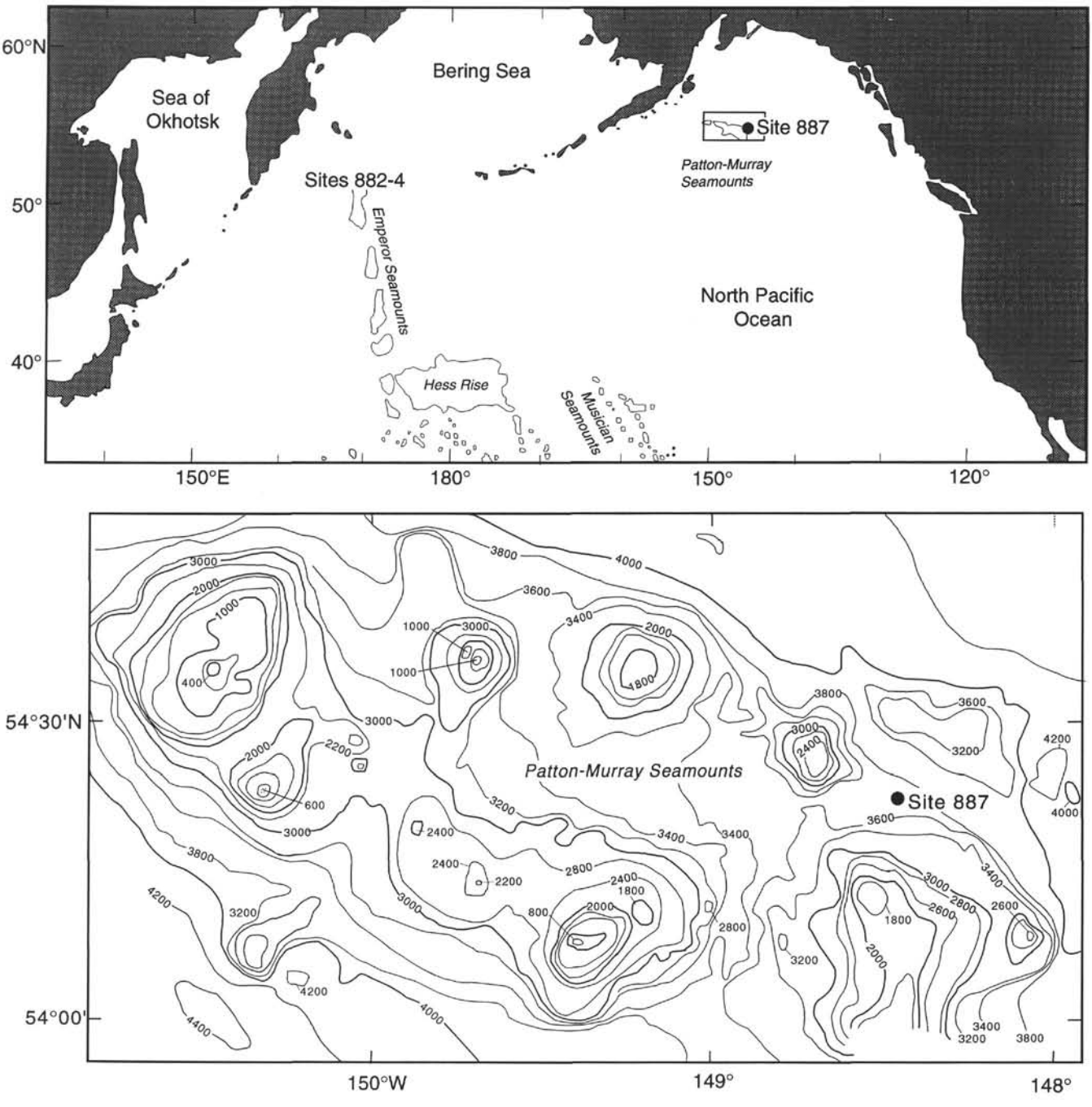

Figure 1. Index map of the North Pacific Ocean indicating the general location of Site 887 and detailed local bathymetry (depths in meters).

ANALYTICAL PROCEDURES

At the UNE, all of the samples were examined under a petrographic microscope to determine the morphologies and sizes of the shards, noting in particular those layers containing a sufficient number of shards large enough to analyze (at least 10 μm in diameter) by electron microprobe (EMP) and any significant organic and clay contamination. We did not sieve any of the samples. Ash samples were carefully washed with distilled water and dried at 105°C, affixed in an epoxy mounting ring, polished, and carbon coated.

The major element chemical compositions of individual vitric shards were obtained at the UNE using a JEOL Model JSM35 EMP with a KEVEX Si-Li energy dispersive spectrometer (EDS). Nine elements (Si, Ti, Al, Fe, Mn, Mg, Ca, K, Na) were analyzed. The shards analyzed appear pristine, with no sign of hydration or clay formation. Standard natural and synthetic glasses from the Smithsonian Institution were analyzed concurrently, with excellent agreement between our analyses and the published values. Furthermore, comparisons of ash analyses obtained with this instrument and wavelength-dispersive EMP (Camebax) at the University of Michigan (Arculus and Bloomfield, 1992) and the Australian National University are in excellent agreement, although we prefer the EDS system for minimizing sample damage and Na loss from hydrous, SiO_2-rich glasses. Operating conditions were 15-kV accelerating voltage, 10-nA beam current, and 100-s count time.

We selected 16 of the 25 ash layers for bulk analysis of 36 trace elements by inductively coupled plasma source mass spectrometry (ICP-MS; using a VG PlasmaQuad PQ2+) at Monash University. Our selection criteria for the application of this analytical technique were

Table 1. Stratigraphic and lithologic characteristics of volcanic ash layers from Hole 887A.

UNE number	Age (Ma)	Depth (mbsf)	Thickness (cm)	Size of vitric shard (0.01 mm)	Color (dry sample)	Color (shipboard estimate)	Composition	Lithology
	0.01	1.5	1	—	—	—	—	Diatom clay and diatom ooze
155	0.02	1.8	5	1 × 5	Light gray (2.5Y 7/1)	—	Rhyolite	Diatom clay and diatom ooze
	0.03	3	6	—	—	—	—	Diatom clay and diatom ooze
	0.04	3.5	3	—	—	—	—	Diatom clay and diatom ooze
	0.04	5.9	3	—	—	—	—	Diatom clay and diatom ooze
	0.05	6.8	5	—	—	—	—	Diatom clay and diatom ooze
	0.09	10.5	1	—	—	—	—	Diatom clay and diatom ooze
156	0.1	10.7	18	2 × 10	Light gray (2.5Y 7/1)	—	Rhyolite	Diatom clay and diatom ooze
157	0.11	11.1	9	2 × 3	Yellowish gray (2.5Y 4/1)	—	—	Diatom clay and diatom ooze
	0.13	11.8	3	—	—	—	—	Diatom clay and diatom ooze
	0.14	12.3	3	—	—	—	—	Diatom clay and diatom ooze
	0.14	12.4	1	—	—	—	—	Diatom clay and diatom ooze
158	0.16	12.8	12	1 × 5	Light gray (2.5Y 8/1)	—	Rhyolite	Diatom clay and diatom ooze
	0.18	13.3	2	—	—	—	—	Diatom clay and diatom ooze
	0.19	13.5	2	—	—	—	—	Diatom clay and diatom ooze
	0.22	13.7	3	—	—	—	—	Diatom clay and diatom ooze
	0.29	14.7	2	—	—	—	—	Diatom clay and diatom ooze
	0.31	16.4	13	—	—	—	—	Diatom clay and diatom ooze
	0.32	17.2	3	—	—	—	—	Diatom clay and diatom ooze
	0.33	19.5	4	—	—	—	—	Diatom clay and diatom ooze
	0.35	20.7	2	—	—	—	—	Diatom clay and diatom ooze
	0.36	23.5	1	—	—	—	—	Diatom clay and diatom ooze
	0.37	24.5	3	—	—	—	—	Diatom clay and diatom ooze
	0.38	25.5	3	—	—	—	—	Diatom clay and diatom ooze
	0.39	26.6	1	—	—	—	—	Diatom clay and diatom ooze
159	0.42	29.7	4	6 × 12	Dark grayish yellow (2.5Y 4/2)	—	—	Diatom clay and diatom ooze
	0.5	34.3	3	—	—	—	—	Diatom clay and diatom ooze
	0.52	34.4	1	—	—	—	—	Diatom clay and diatom ooze
	0.58	37.2	2	—	—	—	—	Diatom ooze with clay
160	0.6	38.8	4	0.5 × 2	Light gray (2.5Y 7/1)	—	Rhyolite	Diatom ooze with clay
161	0.61	39.5	3	5 × 10	Yellowish gray (2.5Y 4/1)	—	Rhyolite	Diatom ooze with clay
	0.63	40.5	1	—	—	—	—	Diatom ooze with clay
	0.64	40.7	2	—	—	—	—	Diatom ooze with clay
162	0.76	46.3	2	3 × 7	Yellowish gray (2.5Y 5/1)	—	Rhyolite	Clay and diatom ooze
163	0.78	48.7	7	1 × 6	Dark grayish yellow (2.5Y 5/2)	—	Rhyolite	Clay and diatom ooze
	0.79	49.7	1	—	—	—	—	Clay and diatom ooze
	0.81	50.3	1	—	—	—	—	Clay and diatom ooze
164	0.85	52.5	1	6 × 8	Yellowish gray (2.5Y 5/1)	—	—	Clay and diatom ooze
	0.88	54.2	1	—	—	—	—	Clay and diatom ooze
	0.89	54.4	5	—	—	—	—	Clay and diatom ooze
	0.91	56.4	1	—	—	—	—	Clay with quartz
	0.92	56.6	2	—	—	Black (2.2GY 2.7/0.6)	—	Clay with quartz
	0.93	56.9	4	—	—	Black (2.2GY 2.7/0.6)	—	Clay with quartz
165	1	61.2	6	—	Yellowish gray (2.5Y 4/1)	Black (2.2GY 2.7/0.6)	—	Clay with quartz
166	1.15	63	7	1 × 5	Yellowish gray (2.5Y 6/1)	Black (2.2GY 2.7/0.6)	—	Clay with quartz
	1.2	64.8	2	—	—	Brown (3.9Y 2.7/1.0)	—	Clay with quartz
	1.3	65.6	3	—	—	Black (0.8GY 2.9/0.5)	—	Clay with quartz
	1.4	66.3	2	—	—	Black (0.8GY 2.9/0.5)	—	Clay with quartz
167	1.55	67.7	3	—	Light gray (2.5Y 8/1)	Black (0.8GY 2.9/0.5)	—	Clay with quartz
	1.6	68.1	3	—	—	Light gray (2.2Y 4.8/0.8)	—	Clay with quartz
	1.7	70		—	—	Black (0.8GY 2.9/0.5)	—	Clay with quartz
	1.8	72.5		—	—	—	—	Clay with quartz
	1.9	72.8	5	—	—	—	—	Clay with quartz
	2	82.9	2	—	—	Black (0.8GY 2.9/0.5)	—	Clay with ash, clay and diatom ooze
168	2.3	84.1	6	3 × 5	Yellowish gray (2.5Y 4/1)	Gray(3.8Y 4.0/1.2)	Basaltic andesite	Clay with ash, clay and diatom ooze
	2.35	84.8	11	—	—	Black (4.8Y 1.8/0.7)	—	Clay with ash, clay and diatom ooze
	2.4	86.5	3	—	—	Black (4.8Y 1.8/0.7)	—	Clay with ash, clay and diatom ooze
	2.5	87.5	1	—	—	Brown (1.6Y 3.3/2.1)	—	Clay with ash, clay and diatom ooze
	2.6	88.2	1	—	—	Gray (3.8Y 4.0/1.2)	—	Clay with ash, clay and diatom ooze
	2.65	88.5	5	—	—	Gray (3.8Y 4.0/1.2)	—	Clay with ash, clay and diatom ooze
169	2.7	89.1	5	1 × 5	Grayish yellow (2.5Y 6/2)	Gray(3.8Y 4.0/1.2)	Dacite-rhyolite	Clay with ash, clay and diatom ooze
	2.71	89.7	6	—	—	Brown (1.6Y 3.3/2.1)	—	Clay with ash, clay and diatom ooze
	2.72	90.3	4	—	—	Gray (3.8Y 4.0/1.2)	—	Clay with ash, clay and diatom ooze
170	2.73	90.7	4	0.5 × 4	Light gray (2.5Y 7/1)	Black (4.8Y 1.8/0.7)	Dacite-rhyolite	Clay with ash, clay and diatom ooze
	2.79	93.5	7	—	—	Gray (3.8Y 4.0/1.2)	—	Diatom ooze
171	2.86	98.7	3	1 × 7	Light gray (2.5Y 7/1)	Black(1.1Y 3.3/0.6)	Rhyolite	Diatom ooze
172	2.87	99.1	3	1 × 5	Light gray (2.5Y 7/1)	Brown(2.0Y 4.2/0.9)	Rhyolite	Diatom ooze
173	3.7	114.3	10	1 × 15	Yellowish gray (2.5Y 6/1)	Brown(2.0Y 4.2/0.9)	Rhyolite	Diatom ooze
174	3.75	116.7	2	1 × 3	Light gray (2.5Y 7/1)	Red(8.7R 3.1/0.8)	Rhyolite	Diatom ooze
	4	123.9	6	—	—	Brown(4.0Y 2.7/0.9)	—	Diatom ooze
175	4.1	124.7	11	2 × 3	Yellowish gray (2.5Y 6/1)	Black(0.8RP 2.6/0.7)	Andesite	Diatom ooze
	4.3	127.1	3	—	—	Black(0.8RP 2.6/0.7)	—	Diatom ooze
	4.7	135.7	4	—	—	Black	—	Diatom ooze
176	4.85	142.9	4	1 × 5	Light gray (2.5Y 7/1)	Light gray	—	Diatom ooze
177	4.88	143.8	4	1 × 4	Light gray (2.5Y 7/1)	Dark brown (9.9YR 2.4/1.8)	Dacite-rhyolite	Diatom ooze
178	8.85	214.2	6	1 × 5	Yellowish gray (2.5Y 6/1)	Dark brown (9.9YR 2.4/1.8)	Basaltic andesite	Nannofossil ooze
179	10.4	230.7	9	2 × 10	Yellowish gray (2.5Y 6/1)	—	Andesite—rhyolite	Nannofossil ooze
180	14.5	256.9	15	2.5 × 15	—	Dark brown (9.0YR 3.2/1.7)	Rhyolite	Nannofossil ooze

to obtain a spread of ages of ash layers; to avoid clay, diatom, and carbonate contamination as much as possible; and to concentrate on those layers that appeared to be relatively homogenous in terms of major element chemistry as resolved by EMP analysis.

Sample preparation involved digestion of 0.1 ± 0.03 g of distilled water-washed ash sample for 24 to 48 hr in screw-top Teflon bombs at 100°–120°C in a mixture of distilled HF (4 mL) and distilled HNO_3 (2 mL). Sample solutions were slowly dried (with heat lamps) and converted from fluorides to nitrates with additions of concentrated HNO_3. Samples were then taken into solution with 50 g of 2% HNO_3 (made from sub-boiled, distilled concentrated HNO_3 and 18.2 MΩ Millipore H_2O). Aliquots of this solution were run at a total dilution factor of

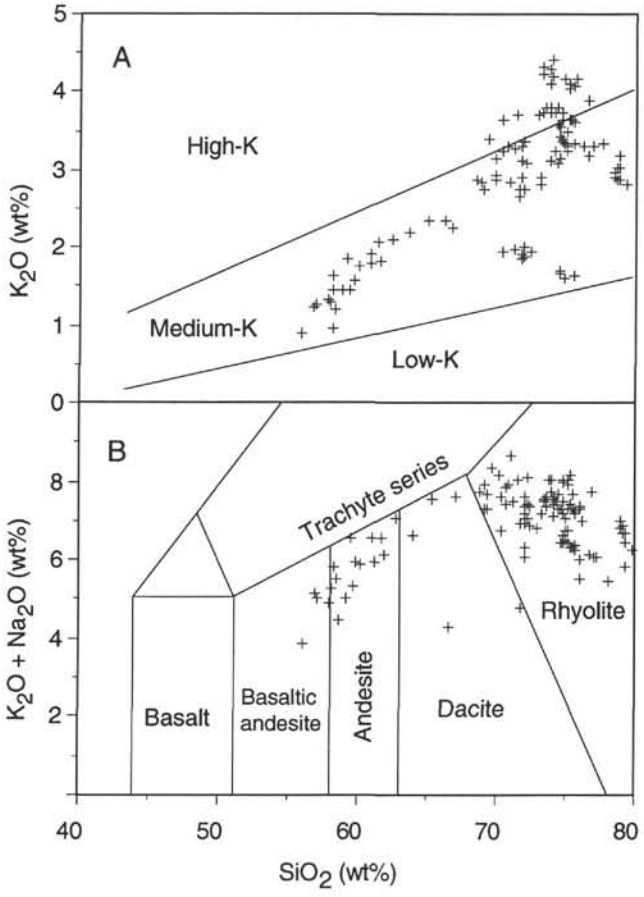

Figure 2. **A.** K_2O vs. SiO_2 for individual vitric shards from Hole 887A. Fields of low-, medium-, and high-K are from Gill (1981). **B.** Variation of (K_2O + Na_2O) vs. SiO_2 for individual vitric shards from Hole 887A. Fields are from Le Bas et al. (1986).

≈2000. All samples were made up with 100 ppb In to serve as an internal standard for drift correction. One analytical blank and five standard solutions (based on U.S. Geological Survey standard rocks) were typically prepared for each run. An initial calibration was performed using synthetic standards and finalized with a set of laboratory and international standards. Total analytical blanks are typically <20 ppb for most elements except for Sc, Cr, Cu, and Ni (which are <500 ppb). Errors are ±15–20 relative% for Sc, Ga, Ge, Pr, Gd, Th, and U depending on abundances, ±5–10 relative% for the other rare earth elements (REE) and ±3–15 relative% for all other trace elements analyzed.

RESULTS

Representative major element analyses of individual vitric shards are listed in Table 2. The bulk analysis of selected ash layers based on the ICP-MS trace element analysis and calculated in the case of major elements from the average of the EMP analyses of individual shards is presented in Table 3.

The composition spectrum of ash layers recovered from Hole 887A ranges from medium-K basaltic andesite to medium- and high-K rhyolite (Fig. 2). No low-K samples were found. Almost all of these samples are tholeiitic on the basis of Miyashiro's (1974) criterion (Fig. 3). An apparent bimodality of compositional distribution of the shards into either andesite or rhyolite groups is apparent in Figures 2 and 3, with minor occurrences of basaltic andesite and dacite compositions. It is not apparent from plots of composition vs. age (Fig. 4) that any regularities of secular change exist, including any trend towards increasingly silicic compositions with time.

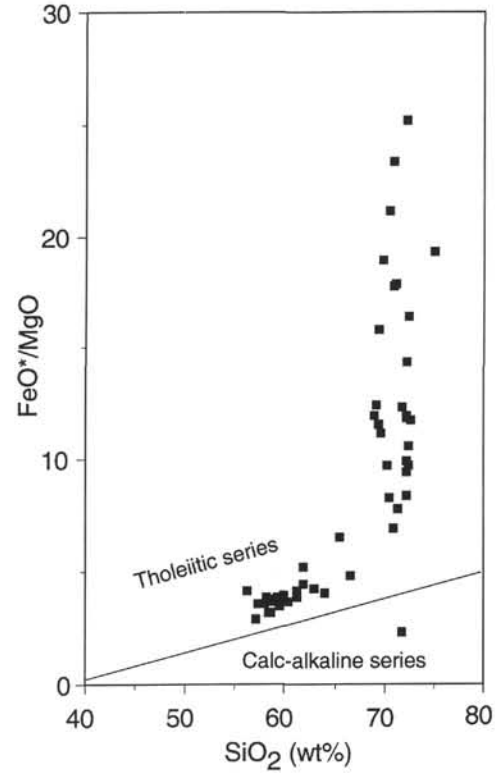

Figure 3. Variation of FeO*/MgO vs. SiO_2 of vitric shards from Hole 887A. The discriminant line between tholeiitic and calc-alkaline series of Miyashiro (1974) is shown.

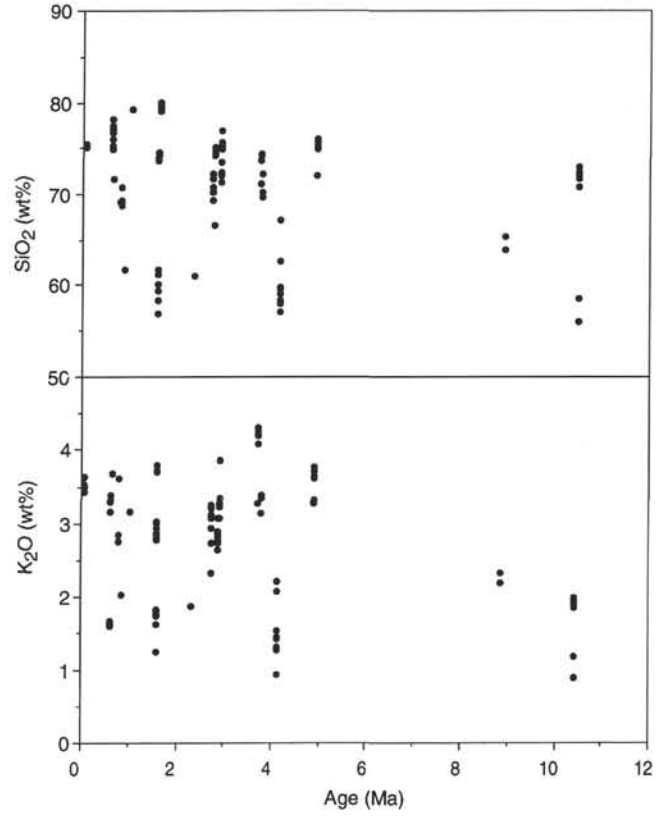

Figure 4. Variation of SiO_2 and K_2O as a function of age of individual vitric shards from Hole 887A. Ages were estimated from shipboard micropaleontology, magnetostratigraphy, and interpolations from the sediment mass-accumulation rate (see text).

Representative chondrite-normalized rare earth element abundances are displayed in Figure 5. A more extended graphical comparison of the abundances of a range of trace elements of variable degrees of crystalline phase compatibility is shown in Figure 6. We note that the abundances of the REE in the majority of these ash samples are similar to those of tholeiitic series volcanic rocks of the Aleutians reported by, for example Kay (1977), with chondrite-normalized La of 40 to 100, Yb of 15 to 30, and La/Yb of about 2 to 3. However, we also note that the chondrite-normalized La/Sm of many of these ash samples (≈2) exceeds that of the tholeiitic rocks of the Aleutian arc and is more similar to the La/Sm fractionation claimed for the calc-alkaline series by Kay (1977). For two of the ash layers (UNE numbers 164 and 165), the REE abundances are similar overall to the calc-alkaline series recognized by Kay (1977). Finally, we note that the distinctively high Ba/Nb and Sm/Ti of the ashes from Site 887 (Fig. 6) are consistent with derivation from an arc magma source.

In summary, on the basis of major and trace element analysis of a representative set of ash layers recovered from Hole 887A, no consistent temporal changes in geochemistry of the sources involved can be discerned for the past ~16 Ma. The range of major element compositions is bimodal with predominant medium-K andesite and medium- to high-K rhyolite groups. Almost all are tholeiitic on the basis of Miyashiro's (1974) criterion. Morphologies of the shards coupled with distinctively high Ba/Nb and Sm/Ti indicate derivation through plinian fallout from explosive eruptions of an island arc. A major increase in the number of ash layers occurs in sediments younger than 2.7 Ma.

ACKNOWLEDGMENTS

The support of David Rea for our involvement in this study is greatly appreciated, as is the diligence of the shipboard scientific party in providing representative samples. Our research was funded by a grant from the Australian Research Council. Peter Garlick and Rick Porter ensured that the EMP at UNE was available and functional. The tolerance and good service of Dr. David Lambert at the Monash ICP-MS facility is much appreciated. L.-Q. Cao was supported by OPRS and UNEOSS scholarships.

REFERENCES*

Arculus, R.J., and Bloomfield, A.L., 1992. Major-element geochemistry of ashes from Sites 782, 784, and 786 in the Bonin forearc. *In* Fryer, P., Pearce, J.A., Stokking, L.B., et al., *Proc. ODP, Sci. Results,* 125: College Station, TX (Ocean Drilling Program), 277–292.

Baker, D.R., and Eggler, D.H., 1983. Fractionation paths of Atka (Aleutians) high-alumina basalts: constraints from phase relations. *J. Volcanol. Geotherm. Res.,* 18:387–404.

Brophy, J.G., 1989. Can high-alumina arc basalt be derived from low-alumina arc basalt? Evidence from Kanaga island, Aleutian arc, Alaska. *Geology,* 17:333–336.

Brophy, J.G., and Marsh, B.D., 1986. On the origin of high-alumina arc basalt and the mechanics of melt extraction. *J. Petrol.,* 27:763–789.

Cambray, H., Cadet, J-P., and Pouclet, A., 1993. Ash layers in deep-sea sediments as tracers of arc volcanic activity: Japan and Central America as case studies. *The Island Arc,* 2:72–86.

Carey, S., and Sigurdsson, H., 1980. The Roseau ash: deep-sea tephra deposits from a major eruption on Dominica, Lesser Antilles arc. *J. Volcanol. Geotherm. Res.,* 7:67–86.

Coats, R.R., 1962. Magma type and crustal structure in the Aleutian arc. *In* Macdonald, G.A., and Kuno, H. (Eds.), *The Crust of the Pacific Basin.* Geophys. Monogr., Am. Geophys. Union, 6:92–109.

Creager, J.S., Scholl, D.W., et al., 1973. *Init. Repts. DSDP,* 19: Washington (U.S. Govt. Printing Office).

Edsall, D.W., 1976. Trace elements in tephra as indicators of magmatic composition in the Aleutian arc. *Geol. Soc. Am. Bull.,* 87:1269–1272.

Geist, E.L., Childs, J.R., and Scholl, D.W., 1988. The origin of summit basins of the Aleutian Ridge: implications for block rotation of an arc massif. *Tectonics,* 7:327–341.

Gill, J.B., 1981. *Orogenic Andesites and Plate Tectonics:* New York (Springer-Verlag).

Gust, D.A., and Perfit, M.R., 1987. Phase relations of a high-Mg basalt from the Aleutian island arc: implications for primary island arc basalts and high-Al basalts. *Contrib. Mineral. Petrol.,* 97:7–18.

Kay, R.W., 1977. Geochemical constraints on the origin of Aleutian magmas. *In* Talwani, M., and Pittman, W.C. III (Eds.), *Island Arcs, Deep Sea Trenches and Back Arc Basins:* Am. Geophys. Union, Maurice Ewing Ser., 1:229–242.

————, 1978. Aleutian magnesian andesites: melts from subducted Pacific ocean crust. *J. Volcanol. Geotherm. Res.,* 4:117–132.

Kay, S.M., Kay, R.W., and Citron, G.P., 1982. Tectonic controls on tholeiitic and calc-alkaline magmatism in the Aleutian arc. *J. Geophys. Res.,* 87:4051–4072

Kay, S.M., and Kay, R.W., 1985. Role of crystal cumulates and the oceanic crust in the formation of the lower crust of the Aleutian arc. *Geology,* 13:461–464.

Le Bas, M.J., Le Maitre, R.W., Streckeisen, A., and Zanettin, B., 1986. A chemical classification of volcanic rocks based on the total alkali-silica diagram. *J. Petrol.,* 27:745–750.

Marsh, B.D., 1979. Island-arc volcanism. *Am. Sci.,* 67:161–172.

Marsh, B.D., and Carmichael, I.S.E., 1974. Benioff Zone magmatism. *J. Geophys. Res.,* 79:1196–1206.

Miller, D.M., Langmuir C.H., Doldstein, S.L. and Franks, A.L., 1992. The importance of parental magma composition of calc-alkaline and tholeiitic evolution: evidence from Umnak Island in the Aleutians. *J. Geophys. Res.,* 97:321–345

Miyashiro, A., 1974. Volcanic rock series in island arcs and active continental margins. *Am. J. Sci.,* 274:321–355.

Morris, J.D., and Hart, S.R., 1983. Isotopic and incompatible element constraints on the genesis of island arc volcanics from Cold Bay and Amak islands, Aleutians, and implications for mantle structure. *Geochim. Cosmochim. Acta,* 47:2015–2030.

Myers, J.D., 1988. Possible petrogenetic relations between low- and high-MgO Aleutian basalts. *Geol. Soc. Am. Bull.,* 100:1040–1053.

Myers, J.D., Marsh, B.D., and Sinha, A.K., 1985. Strontium isotopic and selected trace element variations between two Aleutian volcanic centers (Adak and Atka): implications for the development of arc volcanic plumbing systems. *Contrib. Mineral. Petrol.,* 91:221-234.

Nye, C.J., and Reid, M.R., 1986. Geochemistry of primary and least fractionated lavas from Okmok volcano, central Aleutians: implications for magmagenesis. *J. Geophys. Res.,* 91:10271–10287.

Nye, C.J., and Turner, D.L., 1990. Petrology, geochemistry and age of the Spurr volcanic complex, eastern Aleutian arc. *Bull. Volcanol.,* 52:205–226.

Rea, D.K., Basov, I.A., Janecek, T.R., Palmer-Julson, A., et al., 1993. *Proc. ODP, Init. Repts.,* 145: College Station, TX (Ocean Drilling Program).

Romick, J.D., Perfit, M.R., Swanson, S.E. and Shuster, R.D., 1990. Magmatism in the eastern Aleutian arc: temporal characteristic of igneous activity on Akutan Island. *Contrib. Mineral. Petrol.,* 104:700–720.

Scheidegger, K.F., Corliss, J.B., Jezek, P.A., and Ninkovich, D., 1980. Composition of deep-sea ash layers derived from north Pacific volcanic arcs: variations in time and space. *J. Volcanol. Geotherm. Res.,* 7:107–137.

Scheidegger, K.F., and Kulm, L.D., 1975. Late Cenozoic volcanism in the Aleutian arc: information from ash layers in the northeastern Gulf of Alaska. *Geol. Soc. Am. Bull.,* 86:1407–1412.

Singer, B.S., and Myers, J.D., 1990. Intra-arc extension and magmatic evolution in the central Aleutian arc, Alaska. *Geology,* 18:1050–1053.

Singer, B.S., Myers, J.D., and Frost, C.D., 1992. Mid-Pleistocene basalt from the Seguam volcanic center, central Aleutian arc, Alaska: local lithospheric structures and source variability in the Aleutian arc. *J. Geophys. Res.,* 97:4561–4578.

Sun, S.-S., and McDonough, W.F., 1989. Chemical and isotopic systematics of oceanic basalts: implications for mantle composition and processes. *In* Saunders, A.D., and Norry, M.J. (Eds.), *Magmatism in the Ocean Basins.* Geol. Soc. Spec. Publ. London, 42:313–345.

* Abbreviations for names of organizations and publications in ODP reference lists follow the style given in *Chemical Abstracts Service Source Index* (published by American Chemical Society).

Date of initial receipt: 26 April 1994
Date of acceptance: 31 October 1994
Ms 145SR-127

Table 2. Representative analyses of vitric shards from Hole 887A.

UNE number:	155	155	155	155	155	156	156	156	156	156	156	158	158	158	158
Core, section:	1H-2	1H-2	1H-2	1H-2	1H-2	2H-3	2H-3	2H-3	2H-3	2H-3	2H-3	2H-5	2H-5	2H-5	2H-5
Interval (cm):	36–37	36–37	36–37	36–37	36–37	117–118	117–118	117–118	117–118	117–118	117–118	10–11	10–11	10–11	10–11
SiO_2	75.04	74.96	75.04	75.67	75.27	73.86	74.33	74.47	74.11	74.03	74.77	79.48	79.14	79.36	80.05
TiO_2	0.24	0.21	0.24	0.13	0.14	0.19	0.26	0.19	0.19	0.23	0.23	0.19	0	0	0
Al_2O_3	13.59	13.68	13.83	13.38	13.55	14.06	14.23	14.23	14.19	13.96	13.99	12.32	12.39	12.22	12.02
FeO*	1.87	2	2.18	2.05	2	2.44	2.3	2.33	2.52	2.36	2.53	0.76	0.86	0.87	0.78
MnO	0	0	0	0	0	0	0	0	0	0	0	0	0	0	0
MgO	0	0	0	0	0	0	0	0	0	0	0	0	0	0	0
CaO	1.22	1.16	1.19	1.13	1.16	1.41	1.26	1.28	1.29	1.36	1.2	0.81	0.83	0.89	0.89
K_2O	3.55	3.59	3.44	3.49	3.64	3.74	3.81	3.72	3.8	3.81	3.74	2.87	2.96	2.88	2.81
Na_2O	4.49	4.4	3.72	4.16	4.25	4.31	3.79	3.77	3.9	4.24	3.54	3.57	3.83	3.78	3.46
Total	98.28	104.2	99.15	100.12	100.57	101.21	101.53	98.88	101.68	100.83	98.13	101.72	97	97.36	95.1

UNE number:	158	158	158	158	160	160	160	160	160	160	160	160	160	160	161
Core, section,	2H-5	2H-5	2H-5	2H-5	5H-3	5H-3	5H-3	5H-3	5H-3	5H-3	5H-3	5H-3	5H-3	5H-3	5H-3
Interval (cm):	10–11	10–11	10–11	10–11	67–68	67–68	67–68	67–68	67–68	67–68	67–68	67–68	67–68	67–68	132–133
SiO_2	79.98	79.43	79.15	79.32	76.14	75.1	75.06	75.38	75.29	76.17	77.48	76.82	78.26	77.27	71.88
TiO_2	0	0	0	0	0.28	0.2	0.37	0.33	0.41	0.26	0.24	0.32	0.28	0.23	0.16
Al_2O_3	12.23	12.34	12.2	12.2	13.98	14.07	14.09	14.09	13.28	13.35	13.51	13.81	13.38	13.56	17.07
FeO*	0.78	0.68	0.79	0.79	2.07	1.93	2.14	1.88	1.71	1.74	1.59	1.68	1.65	1.73	4.22
MnO	0	0	0	0	0	0	0	0	0	0	0	0	0	0	0
MgO	0	0	0	0	0	0	0	0	0	0	0	0	0	0	1.86
CaO	0.77	0.86	0.86	0.84	2.01	1.95	1.91	1.88	1.27	1.12	1.11	1.24	1.01	1.14	0
K_2O	2.8	3.04	2.89	3.02	1.65	1.67	1.69	1.62	3.4	3.33	3.3	3.3	3.33	3.17	3.7
Na_2O	3.44	3.65	4.11	3.83	3.86	5.09	4.75	4.82	4.63	4.02	2.77	2.83	2.1	2.9	1.11
Total	94.78	94.95	96.98	98.47	97.33	97.65	98.01	97.39	103.67	101.98	95.63	96.29	94.59	97.01	93.38

UNE number:	162	163	163	163	163	164	165	165	165	168	168	169	169	169	169
Core, section,	6H-2	6H-3	6H-3	6H-3	6H-3	6H-6	7H-5	7H-5	7H-5	10H-1	10H-1	10H-5	10H-5	10H-5	10H-5
Interval (cm):	8–9	98–99	98–99	98–99	98–99	28–29	101–102	101–102	101–102	141–142	141–142	52–55	52–55	52–55	52–55
SiO_2	69.34	68.93	69.23	69.52	70.83	61.81	70.4	79.4	74.62	61.18	53.48	70.42	70.95	71.75	72.26
TiO_2	0.65	0.67	0.67	0.55	0.48	1.16	0.74	0.23	0.33	1.04	1.2	0.5	0.56	0.4	0.54
Al_2O_3	15.13	15.25	15.34	15.06	14.98	16.36	15.66	11.67	14.19	16.34	19.88	15.2	14.7	14.74	15.12
FeO*	4.26	4.43	4.36	4.37	3.74	7.55	3.67	1.47	1.99	7.8	8.62	3.8	3.72	3.39	3.77
MnO	0	0	0	0	0	0	0	0	0	0	0	0	0	0	0
MgO	0.27	0.37	0.35	0.39	0.16	1.44	0.44	0	0	1.87	2.17	0.18	0.21	0	0.15
CaO	2.42	2.62	2.73	2.47	1.95	5.13	2.38	1.4	1.22	5.21	10.34	2.26	1.96	1.7	1.82
K_2O	2.85	2.87	2.85	2.76	3.63	2.06	2.87	3.17	4.41	1.9	0.87	2.94	3.23	3.26	3.12
Na_2O	5.07	4.85	4.47	4.88	4.25	4.49	3.85	2.65	3.24	4.67	3.43	4.69	4.67	4.75	3.21
Total	99.42	99.89	100.31	95.89	97.34	100	100.01	99.99	100	103.13	102.15	103.72	104.25	96.73	95.33

UNE number:	169	169	170	170	170	170	170	170	171	171	171	171	171	171	171
Core, section,	10H-5	10H-5	10H-6	10H-6	10H-6	10H-6	10H-6	10H-6	11H-5	11H-5	11H-5	11H-5	11H-5	11H-5	11H-5
Interval (cm):	52–55	52–55	46–47	46–47	46–47	46–47	46–47	46–47	41–43	41–43	41–43	41–43	41–43	41–43	41–43
SiO_2	78.95	69.47	74.32	66.7	67.54	75.15	74.96	74.72	72.2	73.6	72.41	72.16	73.63	74.96	72.13
TiO_2	0	0.49	0.46	1.36	0	0.32	0.4	0.53	0.47	0.32	0.57	0.65	0.39	0.39	0.38
Al_2O_3	11.99	15.68	14.51	17.73	19.64	14.47	14.53	14.64	15.15	14.65	14.84	14.85	14.51	14.01	15.03
FeO*	1.27	4.18	1.78	3.59	0.16	2.03	1.92	2.09	2.3	2.2	2.53	2.69	2.19	1.82	2.65
MnO	0	0	0	0	0	0	0	0	0	0	0	0	0	0	0
MgO	0	0.36	0	0.74	0	0	0	0	0.16	0	0.26	0.27	0	0	0.28
CaO	0.2	2.56	1.51	5.55	1.18	1.53	1.58	1.56	2.13	1.76	1.95	2.18	1.76	1.33	2.18
K_2O	4.57	2.75	3.12	2.34	4.32	3.14	3.09	3.23	2.89	2.81	2.76	2.75	2.91	3.09	2.65
Na_2O	3.02	4.52	4.3	1.98	7.15	3.35	3.52	3.24	4.7	4.65	4.68	4.45	4.62	4.4	4.69
Total	95.1	98.05	95.72	95.24	103.77	95.49	96.86	96.29	96.99	96.31	99.59	99.04	97.37	97.52	99.25

UNE number:	171	172	172	172	172	172	173	173	173	173	173	174	174	174	174
Core, section,	11H-5	11H-5	11H-5	11H-5	11H-5	11H-5	13H-3	13H-3	13H-3	13H-3	13H-3	13H-4	13H-4	13H-4	13H-4
Interval (cm):	41–43	89–91	89–91	89–91	89–91	89–91	7–8	7–8	7–8	7–8	7–8	97–98	97–98	97–98	97–98
SiO_2	71.36	75.68	72.58	75.53	75.31	77.11	74.34	74.33	74.56	73.84	73.84	71.18	72.43	69.86	70.3
TiO_2	0.56	0.39	0.58	0.33	0.52	0.28	0.18	0.24	0.2	0.35	0.38	0.41	0.26	0.55	0.49
Al_2O_3	15.32	13.43	14.34	13.56	13.77	12.92	14.69	14.32	14.63	14.53	14.44	15.23	15.25	15.59	15.55
FeO*	2.66	2.02	2.82	1.93	1.89	1.21	2.52	2.38	2.19	2.68	2.57	2.86	2.68	3.41	3.21
MnO	0	0	0	0	0	0	0	0	0	0	0	0	0	0	0
MgO	0.34	0	0.24	0	0	0	0	0	0	0	0	0.16	0	0.18	0.33
CaO	2.26	1.17	2.03	1.2	1.23	0.73	1.15	1.16	1.13	1.24	1.17	1.51	1.28	2.05	1.97
K_2O	2.85	3.25	3.08	3.29	3.35	3.88	4.28	4.1	4.21	4.24	4.32	3.29	3.35	3.39	3.16
Na_2O	4.66	4.06	4.31	4.16	3.93	3.87	2.84	3.45	3.09	3.13	3.29	5.37	4.74	4.97	5.01
Total	99.14	102.55	98.7	96.52	96.79	97	95.44	96.93	95.97	96.92	98.18	95.87	93.95	95.44	95.94

Table 2 (continued).

UNE number:	175	175	175	175	175	175	175	175	175	175	177	177	177	177	177
Core, section,	14H-3	14H-3	14H-3	14H-3	14H-3	14H-3	14H-3	14H-3	14H-3	14H-3	16X-3	16X-3	16X-3	16X-3	16X-3
Interval (cm):	97–98	97–98	97–98	97–98	97–98	97–98	97–98	97–98	97–98	97–98	104–105	104–105	104–105	104–105	104–105
SiO_2	58.48	59.18	58.16	62.87	67.21	57.22	58.03	59.95	59.7	58.49	75.2	75.29	72.24	65.31	75.43
TiO_2	0.96	1.3	1.16	1.03	0.48	1.29	1.2	1.24	1.03	1.2	0.27	0.35	0.57	1.06	0.37
Al_2O_3	17.85	15.72	17.6	16.15	18.73	16.03	16.28	16.82	16.56	16.13	13.65	13.78	14.7	15.74	13.78
FeO*	7.04	9.66	8.22	6.46	1.81	10.31	9.84	7.91	8.47	9.34	2.29	2.32	3.36	5.56	2.4
MnO	0	0	0	0	0	0	0	0	0	0	0	0	0	0	0
MgO	2.18	2.51	2.14	1.51	0	2.86	2.75	2.01	2.3	2.54	0	0	0.4	1.52	0
CaO	7.99	6.64	7.44	4.93	4.19	7.27	7.02	6.11	6.63	6.79	1.55	1.54	2.65	4.64	1.73
K_2O	0.95	1.46	1.3	2.09	2.24	1.28	1.33	1.56	1.44	1.46	3.72	3.73	3.29	2.37	3.33
Na_2O	4.55	3.54	3.98	4.96	5.34	3.76	3.55	4.39	3.88	4.06	3.31	3	2.79	3.81	2.97
Total	104.66	102.65	101.09	101.08	101.3	102.12	102.34	101.84	100.34	102.49	103.04	95.52	96.71	99.58	95.48

UNE number:	177	177	177	177	177	178	178	178	179	179	179	179	179	179	179
Core, section,	16X-3	16X-3	16X-3	16X-3	16X-3	24H-2	24H-2	24H-2	25H-6	25H-6	25H-6	25H-6	25H-6	25H-6	25H-6
Interval (cm):	104–105	104–105	104–105	104–105	104–105	24–25	24–25	24–25	97–98	97–98	97–98	97–98	97–98	97–98	97–98
SiO_2	75.92	76.19	75.74	74.96	75.77	65.52	64.01	53.82	72.25	72.43	58.67	70.89	71.82	73	72.49
TiO_2	0.25	0.31	0.33	0.79	0.46	1.03	1.34	2.58	0.52	0.48	1.73	0.74	0.75	0.45	0.59
Al_2O_3	13.68	13.79	13.93	12.8	13.7	15.4	15.76	16.36	14.29	14.19	15.73	13.98	13.97	14.33	14.4
FeO*	2.39	2.25	2.19	3.28	2.22	5.86	6.39	11.08	3.57	3.49	9.39	4.1	4.19	3.59	3.45
MnO	0	0	0	0	0	0.19	0	0	0	0	0	0	0	0	0
MgO	0	0	0	0.17	0	0.89	1.56	3.72	0.3	0.33	2.93	0.59	0.34	0	0.21
CaO	1.48	1.45	1.5	1.57	1.49	3.6	4.3	8.56	2.05	2.02	7.09	2.3	2.01	1.86	1.97
K_2O	3.63	3.62	3.64	3.79	3.64	2.34	2.2	1	1.91	1.88	1.2	1.95	1.97	1.95	2
Na_2O	2.65	2.4	2.67	2.64	2.72	5.18	4.44	2.87	5.12	5.19	3.25	5.45	4.95	4.83	4.89
Total	97	95.55	96.6	96.52	97.04	103.42	100.52	104.04	103.02	101.04	101.74	100.61	99.35	97.11	97.52

UNE number:	179	179	180	180	180	180	180	180	180
Core, section,	25H-6	25H-6	28H-5	28H-5	28H-5	28H-5	28H-5	28H-5	28H-5
Interval (cm):	97–98	97–98	22–23	22–23	22–23	22–23	22–23	22–23	22–23
SiO_2	72.27	56.14	75.47	73.46	75.86	75.84	76.13	76.32	69.88
TiO_2	0.55	1.87	0.26	0.37	0.24	0.21	0.31	0.38	1.11
Al_2O_3	14.34	15.54	13.46	14.82	13.83	13.94	13.64	13.69	12.88
FeO*	3.58	11.16	1.8	2.5	1.87	1.78	1.71	1.7	6.82
MnO	0	0	0	0	0	0	0	0	0
MgO	0.3	2.72	0	0	0	0	0	0	0.69
CaO	2.05	8.74	0.87	1.7	1	0.99	0.94	0.91	1.22
K_2O	1.86	0.91	4.18	3.71	4.04	4.09	4.07	4.18	2.49
Na_2O	5.05	2.93	3.97	3.44	3.16	3.14	3.21	2.82	4.9
Total	98.38	100.01	98.62	96.59	92.02	95.4	97.01	95.64	101.46

Notes: Major elements reported as wt% oxides. UNE number = ash-layer number analyzed at the University of New England (see Table 1). Total = original analytical total. Individual oxide values sum to 100%. Zero values indicate that the element abundances are less than the detection limit of EDS.

Table 3. Bulk major and trace element analyses of ash layers from Hole 887A.

UNE number:	160	163	164	165	168	169	170	171	172	173	174	175	177	178	179	180
Core, section:	5H-3	6H-3	6H-6	7H-5	10H-1	10H-5	10H-6	11H-5	11H-5	13H-3	13H-4	14H-3	16X-3	24H-2	25H-6	28H-5
Interval (cm):	67–68	98–99	28–29	101–102	141–142	52–55	46–47	41–43	89–91	7–8	97–98	63–64	104–105	24–25	121–122	22–23
SiO_2	76.39	69.63	61.81	74.81	57.33	72.3	72.23	72.81	75.24	74.18	70.94	59.93	74.21	61.12	68.88	74.71
TiO_2	0.29	0.59	1.16	0.43	1.12	0.42	0.51	0.47	0.42	0.27	0.43	1.09	0.48	1.65	0.85	0.41
Al_2O_3	13.7	15.16	16.36	13.84	18.11	14.57	15.92	14.8	13.6	14.52	15.41	16.79	13.96	15.84	14.53	13.75
FeO*	1.8	4.23	7.55	2.38	8.21	3.36	1.93	2.38	1.97	2.47	3.04	7.91	2.83	7.78	5.17	2.6
MnO	0	0	0	0	0	0	0	0	0	0	0	0	0	0.06	0	0
MgO	0	0.32	1.44	0.15	2.02	0.15	0.12	0.16	0.05	0	0.17	2.08	0.21	2.06	0.86	0.1
CaO	1.43	2.44	5.13	1.67	7.78	1.75	2.15	1.94	1.27	1.17	1.7	6.5	1.96	5.49	3.34	1.09
K_2O	2.69	3.03	2.06	3.48	1.39	3.31	3.21	2.84	3.37	4.23	3.3	1.51	3.48	1.85	1.74	3.82
Na_2O	3.7	4.61	4.49	3.25	4.05	4.14	3.92	4.61	4.07	3.16	5.02	4.2	2.9	4.16	4.63	3.52
Sc	16	15	13	13	24	14	8	14	12	12	13	22	11	17	18	10
V	44	38	89	108	164	40	52	34	37	32	46	177	12	44	72	29
Cr	14	8	46	60	9	7	37	7	7	9	7	11				s
Co	3	7	11	17	17	5		4	3	5	7	37	5	8	8	5
Ni	9	12	25	32	16	6		10	7	10	11	28	2	11	8	5
Cu	22	24	14	13	40	27		13	30	47	16	40	7	22	16	11
Zn	36	56	29	34	72	48		45	42	37	48	60	30	58	54	31
Ga	14	19	12	13	21	18	4	17	17	17	17	18	15	19	18	15
Ge	1	1	1	1	1	1		1	1	1	1	1	1	1	1	1
Rb	26.8	59.7	39	38.8	33.2	58.3	23.3	56.3	62.7	91.3	46.6	22.8	69.7	41.1	20.7	68.9
Sr	259	231.4	343.9	348.4	400.3	201.5	247.2	223.8	197.5	175.8	232	428.6	200.7	244.7	254.5	161.5
Y	35.6	54.4	14.7	16	42.1	53.2	5.4	47.9	47.7	48.9	41.2	30.6	44.3	48.5	42.7	34.7
Zr	145.6	295.7	47	53.3	177.8	294.7	122.3	252.1	271.1	362.9	239.3	142.2	325.5	271.1	208.6	325.7
Nb	3.8	10.3	5.4	6.1	5.7	8.9	4.1	11.4	12.3	10.1	6.8	4.7	9	12.7	10.3	11.7
Cs	0.9	3.5	1.2	1.3	1.6	3.1	0.7	2.3	2.6	4.8	2	0.9	4	2.1	0.9	3.1
Ba	459.6	743.9	602.9	576.2	629.9	862.3	292.3	713.9	683.7	847.8	643.8	428	895.9	526.3	308.9	628.2
La	10.53	22.57	14.54	15.76	16.76	21.51	9.2	20.5	20.72	31.45	17.99	12.56	25.24	19.87	15.45	22.04
Ce	24.74	50.3	29.37	31.51	38.4	48.25	25.51	45.05	45.33	66.42	41.02	29.41	54.26	44.19	35.34	47.3
Pr	3.39	6.8	3.59	3.76	5.48	6.97	2.93	6.38	6.11	8.44	5.88	4.26	7.57	6.51	5.3	6.36
Nd	16.12	31.83	15.15	15.63	26.55	30.65	8.16	27.58	26.58	34.35	26.12	19.35	31.43	29.66	24.61	25.75
Sm	4.34	7.75	3.19	3.32	6.72	7.46	2.11	6.66	6.35	7.53	6.3	4.88	7.17	7.23	6.22	5.53
Eu	1.35	2.21	1.29	1.36	2.28	2.18	0.65	2.11	1.89	1.9	1.95	1.69	2.05	2.13	1.92	1.4
Gd	4.15	8.2	3.7	4.18	6.38	8.27	1.19	7.62	7.02	8.7	6.54	4.73	9.13	7.96	7	7.14
Tb	0.75	1.25	0.44	0.47	1.06	1.23	0.17	1.1	1.05	1.17	0.99	0.77	1.14	1.16	1.02	0.84
Dy	4.64	7.59	2.45	2.58	6.04	7.69	1.02	6.94	6.56	7.09	6.08	4.74	6.82	6.89	6.17	4.97
Dy	5.17	8.09	2.47	2.53	6.39	8.03	1.76	7.3	6.95	7.43	6.4	5.11	6.91	7.15	6.38	4.99
Ho	1.14	1.77	0.51	0.53	1.39	1.76	0.35	1.59	1.53	1.58	1.37	1.08	1.47	1.51	1.38	1.06
Er	3.02	4.63	1.35	1.43	3.61	4.49	0.76	4.01	3.91	4.12	3.52	2.68	3.86	3.95	3.58	2.89
Tm	0.54	0.79	0.21	0.23	0.59	0.77	0.14	0.68	0.67	0.7	0.59	0.45	0.64	0.65	0.58	0.48
Yb	3.34	5.09	1.33	1.47	3.74	5.09	1.09	4.45	4.33	4.49	3.86	2.87	4.22	4.26	3.96	3.28
Lu	0.5	0.78	0.19	0.22	0.56	0.86	0.14	0.75	0.75	0.77	0.65	0.47	0.7	0.68	0.6	0.53
Hf	3.6	7.25	1.1	1.25	4.42	7.6	1.58	6.5	7.04	9.71	6.31	3.86	8.24	6.5	4.98	7.58
Ta	0.3	0.77	0.38	0.42	0.44	0.65	0.35	0.77	0.84	0.78	0.52	0.38	0.7	0.83	0.7	0.86
Pb	5.98	14.6	6.81	6.08	10.24	25.83	3.95	18.93	20.14	22.68	17.12	11.32	23.07	13	7.04	13.74
Th	1.33	5.92	2.74	2.77	1.95	6.19	0.5	5.58	6.35	14.91	5.66	2.03	9.67	3.77	1.62	6.63
U	0.55	2.32	0.83	0.79	0.52	3.68	0.58	3.23	3.64	7.03	3.14	1.1	4.72	1.76	0.8	2.88

Note: UNE number = ash-layer number analyzed at the University of New England (see Table 1). Major elements are averages of individual shard analyses from the same layer. Major elements reported as wt% oxides and trace elements as parts per million. All Fe reported as FeO*.

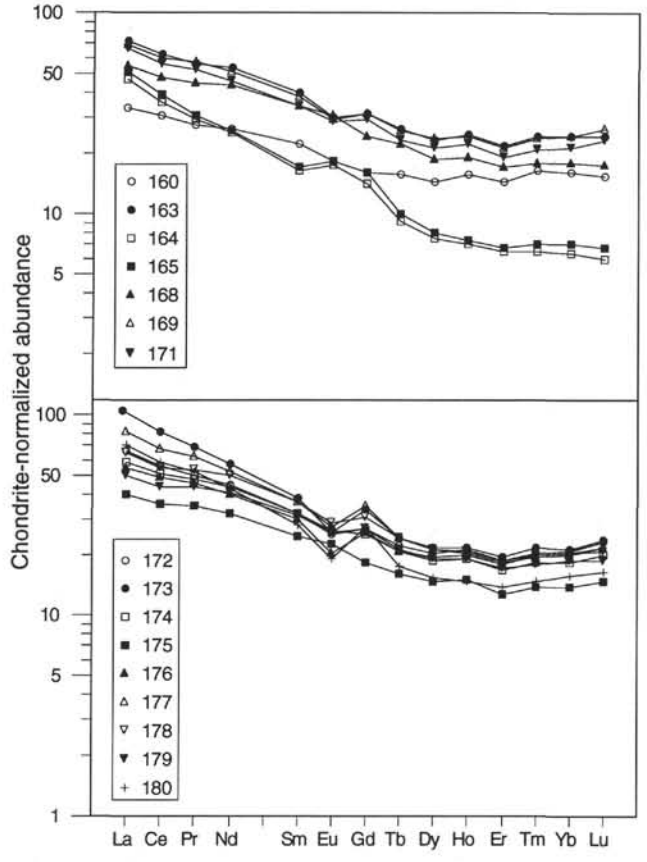

Figure 5. Chondrite-normalized rare earth element abundances for bulk samples of ash layers from Hole 887A. UNE numbers are shown for individual layer symbols (see Table 1).

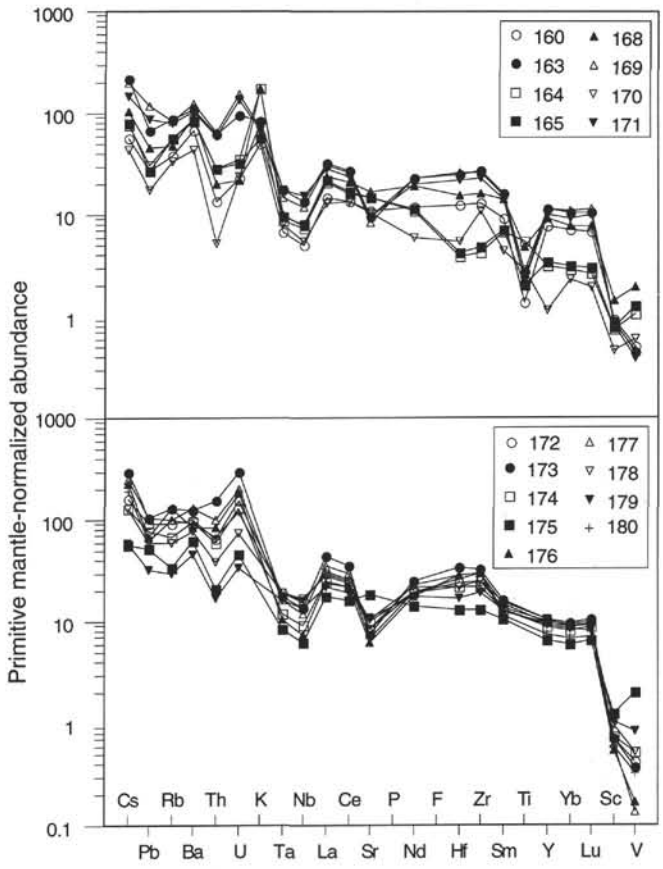

Figure 6. Primitive mantle-normalized trace element abundances for bulk samples of ash layers from Hole 887A. UNE numbers are shown for individual layer symbols. Normalizing values from Sun and McDonough (1989).